Active-Amplifier-Array Diagnostics Using High-Resolution Electrooptic Field Mapping

Kyoung Yang, *Member, IEEE*, Todd Marshall, *Student Member, IEEE*, Michael Forman, *Student Member, IEEE*, John Hubert, Lee Mirth, Zoya Popović, *Senior Member, IEEE*, Linda P. B. Katehi, *Fellow, IEEE*, and John F. Whitaker, *Member, IEEE*

Abstract—Several Ka-band spatial-amplifier power combiners and their free-space feeds were characterized using a high-resolution extreme-near-field electrooptic measurement technique. The two-dimensional electric-field amplitude and phase maps obtained from several arrays are presented. The usefulness of the technique for diagnostic purposes during the design and prototyping stages of the active arrays is discussed. In particular, the electrooptic maps were shown to be valuable for making improvements in the bias line design in one case, and for isolating faulty unit cells in another case.

Index Terms—Electrooptic sampling, near-field radiation patterns, quasi-optical.

I. INTRODUCTION

THE use of microwaves in areas such as satellite communications, wireless and mobile communications, navigation, remote sensing, etc. has led to an extensive effort to produce lightweight high-power alternatives to tube-based microwave amplifiers. In particular, quasi-optical (QO) power-combining amplifier arrays have demonstrated power levels up to 100 W at X-band [1] and 25 W at Ka-band [2]. However, challenges associated with the operation of QO arrays still remain due to the complexity of the designs and the related difficulty in isolating all parasitic high-frequency mechanisms. Thus, reliable diagnostics that are performed in the initial design phase are important for the fundamental understanding of the physical processes in the arrays.

Traditional near- and far-field measurement techniques using waveguides or antennas yield only a limited amount of information on complicated active arrays. These systems, while providing valuable information on the coarse near-field operation

of QO power combining systems, are not able to determine the amplitudes and phases of the electric-field vector components with high resolution across the array. This has prompted the development of an electrooptic field-mapping system [3] that provides high spatial resolution and high measurement bandwidth in order to evaluate the extreme near-electric-field patterns of radiating structures.

A number of electrooptic measurements of antenna near-field patterns have been reported [4], [5]. However, previous work has mainly concentrated on one-dimensional scans or the acquisition of only two field components in the near field, providing limited information on active antenna arrays.

In this paper, extreme-near-field measurements based on the electooptic sampling technique [6], [7] have been performed for two different types of Ka-band QO amplifier arrays. The results have been used in order to evaluate the performance of the arrays and identify important design issues. In the process of conducting the measurements, three different types of horn antenna feeds, which are integral parts of the QO amplifier arrays, have also been characterized. The high resolution and accuracy of the electrooptic field-mapping technique has proven to be advantageous in the design cycle of amplifier arrays, and has diagnosed problems such as nonuniform bias, nonuniform feed amplitude, and malfunctioning monolithic microwave integrated circuits (MMICs).

II. MEASUREMENT SYSTEM CONFIGURATION

The experimental measurement system used for the extreme-near-field characterization of the QO amplifier array structures is shown in Fig. 1. This type of electrooptic sampling system has been introduced previously [3], [8], but is summarized here for completeness. The optical beam from a phase-stabilized Ti : sapphire laser, which has 100-fs duration pulse output at an 80-MHz pulse repetition rate, is focused inside the electrooptic probe crystal [9], [10]. The faces of the probe crystal are polished in order to achieve total internal reflection of the incident beam, which is detected by a photo diode. The reflected beam is analyzed to determine the change of its polarization state, which is sensitive to the magnitude and phase of the RF electric field that extends into the probe crystal. In practice, the laser pulse train passes through a polarizer so that the electrical signal from the photodiode is proportional to the modulated optical intensity. Harmonic mixing of the input

Fig. 1. Electrooptic measurement schematic for near-field mapping of QO amplifier arrays.

Fig. 2. Operational schematic of a planar QO amplifier.

microwave signal frequency and an integer harmonic of the 80-MHz repetition rate of the laser [the local oscillator (LO)] takes place in the electrooptic crystal and is used to obtain an IF that is fed into an RF lock-in amplifier [11], [12]. Using phase-locked-loop electronics in the stabilized laser system, one is able to synchronize the continuous-wave (CW) signal from a microwave synthesizer to the laser pulse train, with the small offset frequency (i.e., the IF) providing the time delay for the sampling gate. Measurements in amplitude and phase are then performed simultaneously as the computer reads the output of the two channels of the lock-in amplifier, which takes the output of a low-frequency synthesizer, also synchronized to the laser electronics, to maintain a phase reference.

The two types of electrooptic probes utilized in this paper are fabricated from bismuth–silicate (BSO) and lithium–tantalate (LiTaO$_3$). These crystals allow the determination of three orthogonal electric-field components above the antenna under test (BSO for the normal field and LiTaO$_3$ for the two tangential fields). Thus, the BSO crystal is utilized to detect the field component that is perpendicular to the plane of a device-under-test (DUT). In order to capture two tangential orthogonal-field components, the LiTaO$_3$ crystal must be rotated about an axis normal to the plane of the DUT between two orientations that are separated by 90°. The crystals have a tip area of 40 μm $\times$ 40 μm for the BSO and 20 μm $\times$ 10 μm for the LiTaO$_3$.

The DUT is mounted on a computer-controlled x–y translation stage, and a typical scan over an array of several square inches takes between 30–60 min, depending on the exact size and desired resolution. The spatial resolution of the field-mapping technique has been demonstrated to be 8 μm, although it is not necessary to scan fields with this level of detail for the measurements described herein. In addition to the two-dimensional movement of the DUT, the optical components allow the probe to have freedom of movement in the vertical direction in order
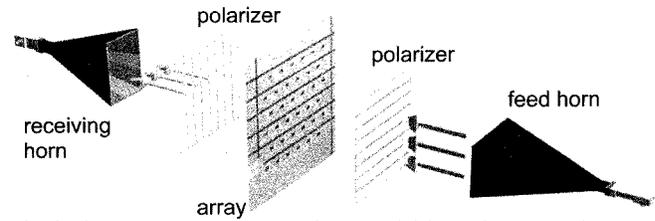
to achieve a three-dimensional field-mapping capability. The minimum detectable voltage is measured to be about 0.5 mV, or −45 dBm, and the sensitivity is 40 mV/$\sqrt{\text{Hz}}$. Furthermore, the isolation between measurements of orthogonal-field components, which is determined by comparing the amplitudes of the components parallel to two orthogonal sides of a patch antenna while using an electrooptic crystal that is aligned for maximum sensitivity to only one of those components, is typically 30 dB. Due to this high cross-polarization-suppression characteristic, electrooptic field mapping does not require any additional polarizing grid to separate one field component from the others.

In terms of the effect that the electrooptic probes have on the field at the probing location (i.e., in terms of the invasiveness of the probe), it is expected that the dielectric crystals will disturb the field pattern much less than a metal waveguide or dipole probe. Nonetheless, the BSO and LiTaO$_3$ probes do have high values of permittivity, in excess of 40 for both crystals and, thus, can be expected to have some influence on local fields [13]. However, it is also true that, in numerous instances for both guided [3], [14] and radiated fields [15], electrooptic measurements have been demonstrated to be in excellent agreement with known or expected field behavior and with computational results. Thus, our confidence in the accuracy of the measurements presented herein is very high.

III. MEASUREMENT RESULTS

The normal operation of a QO array is shown in Fig. 2. A feed antenna radiates a wave that illuminates the feed elements of the active array, thus eliminating the need for a corporate feed. Ideally, each element should receive the same amplitude and phase input, amplify it, and radiate in phase. The goal of free-space power combining is high power-combining efficiency for a large number of elements. The feed can be placed in the far field so that the array is illuminated by a plane wave. This, however, yields low feed efficiency, which can be improved with the use of bulky dielectric lenses. Alternatively, the feed can be placed in the near field, with low associated diffraction loss and improved feed efficiency. This has been done by using specially designed horn antennas ("hard" horns) [16], or by designing the array itself to be a microwave lens, e.g., as in [17]. In the following, QO arrays fed by a hard horn are measured and results are presented and discussed in the context of array performance.

A. Experimental Characterization of Horn Feeds

Before testing the array of interest, it is important to characterize the output field pattern of the feed horns because their aperture distribution strongly affects the near-field pattern ex-
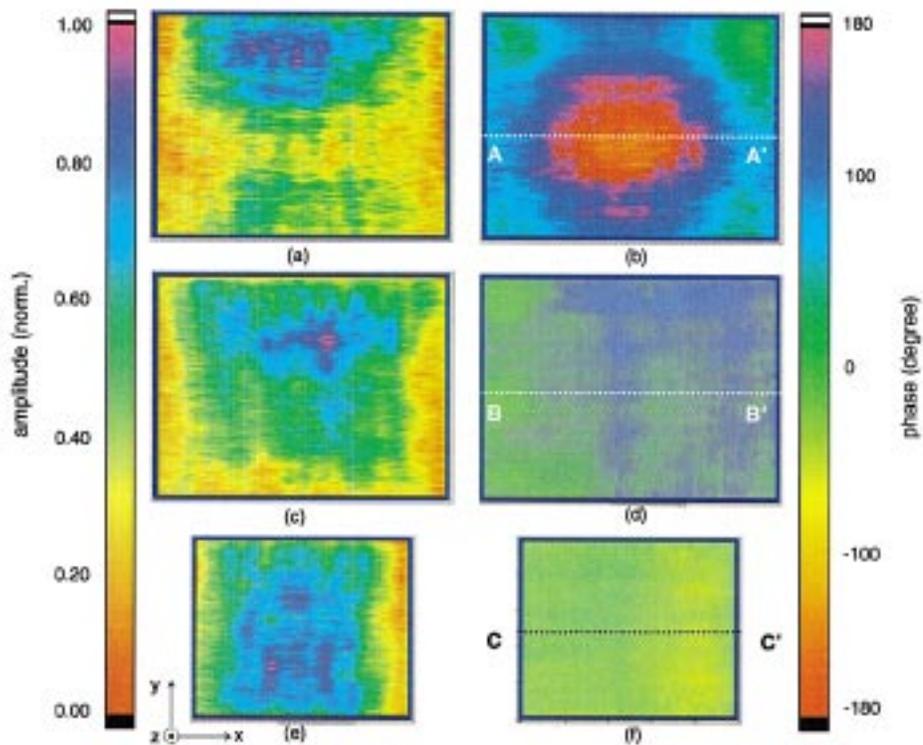
Fig. 3.   Electrooptic measurement results for various horn antennas at $f_{in} = 31$ GHz. (a) Normalized amplitude for standard WR-28 horn and (b) phase (in degrees). (c) Normalized amplitude and (d) phase for hard horn $H1$. (e) Normalized amplitude and (f) phase for hard horn $H2$. The metal boundaries of the horn apertures are overlayed with a bold blue line. The horizontal lines in the phase plots are the locations from which the one-dimensional data in Fig. 4 are derived.
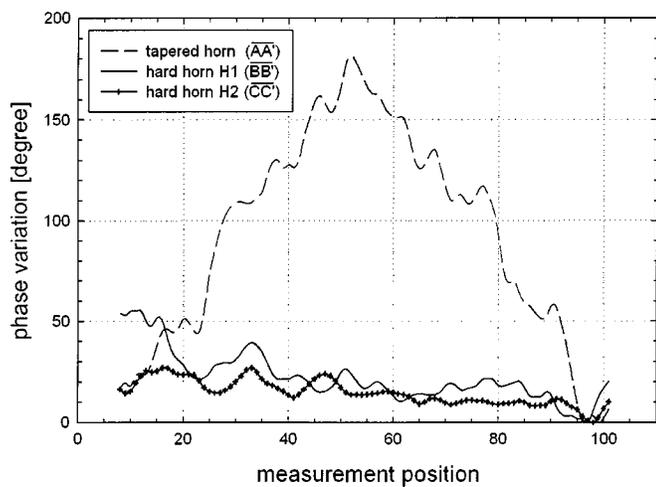

Fig. 4.   One-dimensional phase variations for three horn antennas along the dotted lines shown in the phase plots in Fig. 3. The phase variations are extracted along $\overline{AA}'$ for the standard WR-28 horn, $\overline{BB}'$ for hard horn $H1$, and $\overline{CC}'$ for hard horn $H2$. Measurement position 50 is the center of the aperture.

cited on the array. A standard linear tapered horn and two different types of hard horns were considered as feeds for the arrays. One of the hard horns (labeled $H1$) is based on a standard horn body with inserted dielectric, while the other (labeled $H2$) uses a customized taper, as described in [16]. Dielectric layers on the walls of the hard horns and lenses filling the aperture are used in both cases to achieve uniform phase at a short distance from the opening of the horn [16].
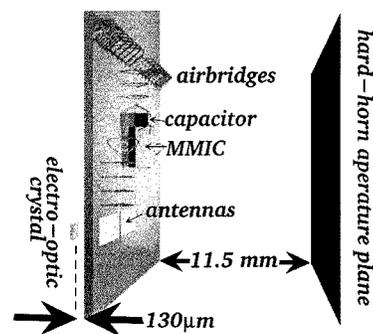
Fig. 5.   Schematic of near-field measurements for arrays A and B; LiTaO$_3$ is used as the electrooptic sensing medium. To display important structures in the array, the drawing is not to scale.
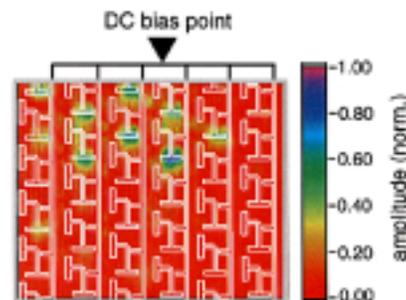

Fig. 6.   Electrooptic field mapping of the normalized amplitude of the QO array with inadequate dc-bias network. The circuit outline is overlayed. The mapping resolution is 500 μm × 450 μm, and the total scan area is 6.25 cm × 4.8 cm.
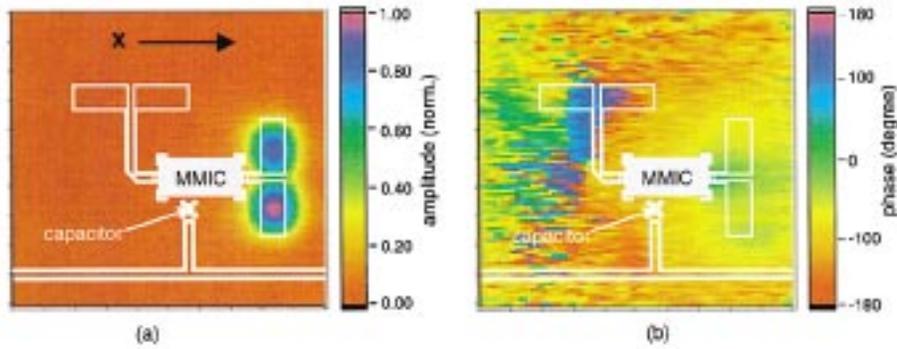
Fig. 7.   Electrooptic scan of a unit cell in array B. (a) Normalized amplitude and (b) phase (in degrees). The scan step size is 93 μm $\times$ 100 μm, and the scan area is 9.3 mm $\times$ 10 mm.
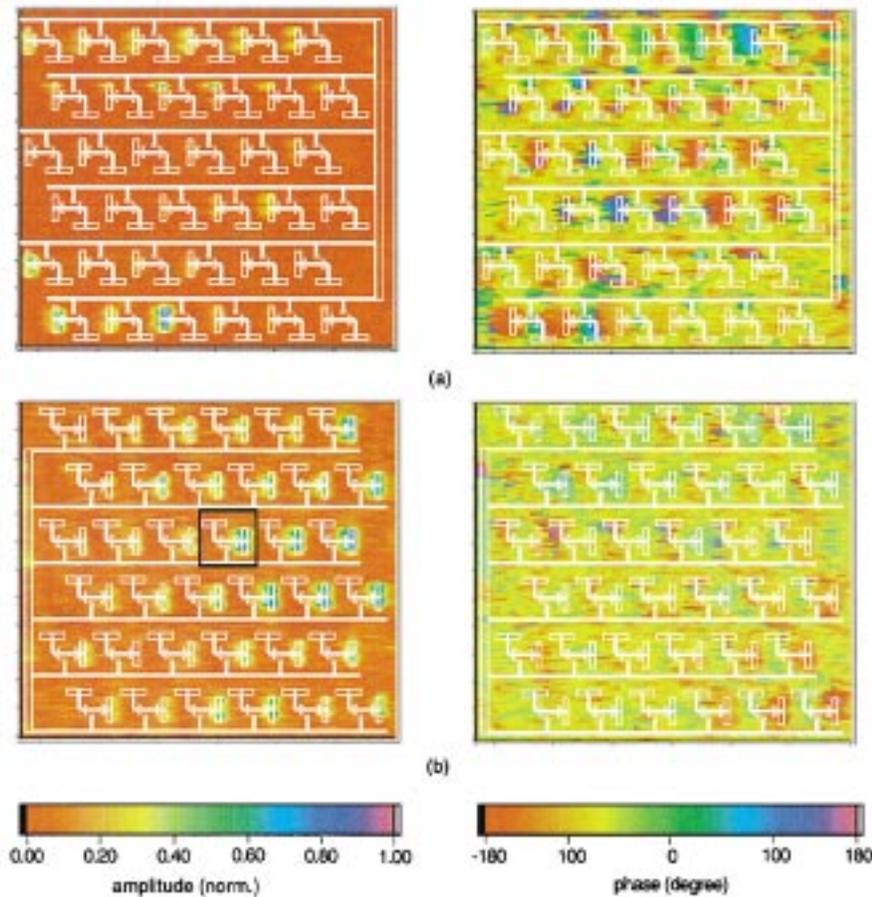

Fig. 8.   Amplitude and phase from electrooptic scan of array. (a) Type A. (b) Type B. The square in array B shows the position of the unit cell from Fig. 7. The scan step size is 500 μm $\times$ 450 μm, and total scan area is 6.3 cm $\times$ 5.4 cm.

The frequency of operation is 31.043 GHz, which is a combination of a 31.04-GHz RF signal (388×80 MHz, the closest integer-multiple frequency of 80 MHz to the operating frequency of the horn antenna) and a 3-MHz IF signal. Due to the limitation of the RF synthesizer used in the measurement (20-GHz maximum output frequency), a frequency doubler generating 31.043-GHz output from a 15.5215-GHz input signal was added between the RF synthesizer output port and the input port of the horn antennas. Fig. 3(a) and (b) shows the normalized amplitude and phase of the dominant electric field component (i.e., the y-component) for the standard linear tapered horn. The phase measurement displays a 180° phase variation from the center to

the edge of the aperture, which agrees well with theoretical predictions for this horn output [18]. Fig. 3(c) and (d) displays the normalized amplitude and phase of the y-component of the electric field for horn $H1$. In comparison with a standard horn, the results show significant improvement in the uniformity of the phase [see Fig. 3(d)]. This phase variation for horn $H1$ is around 50°. The horn $H2$ shows the most uniform amplitude and phase distribution of the electric field [see Fig. 3(e) and (f)]—there is only a 20° phase variation measured across the aperture, and the amplitude distribution is within 10 dB. The phase variation across each of the horns is more easily extracted from one-dimensional phase maps, as shown in Fig. 4. Based on these mea-
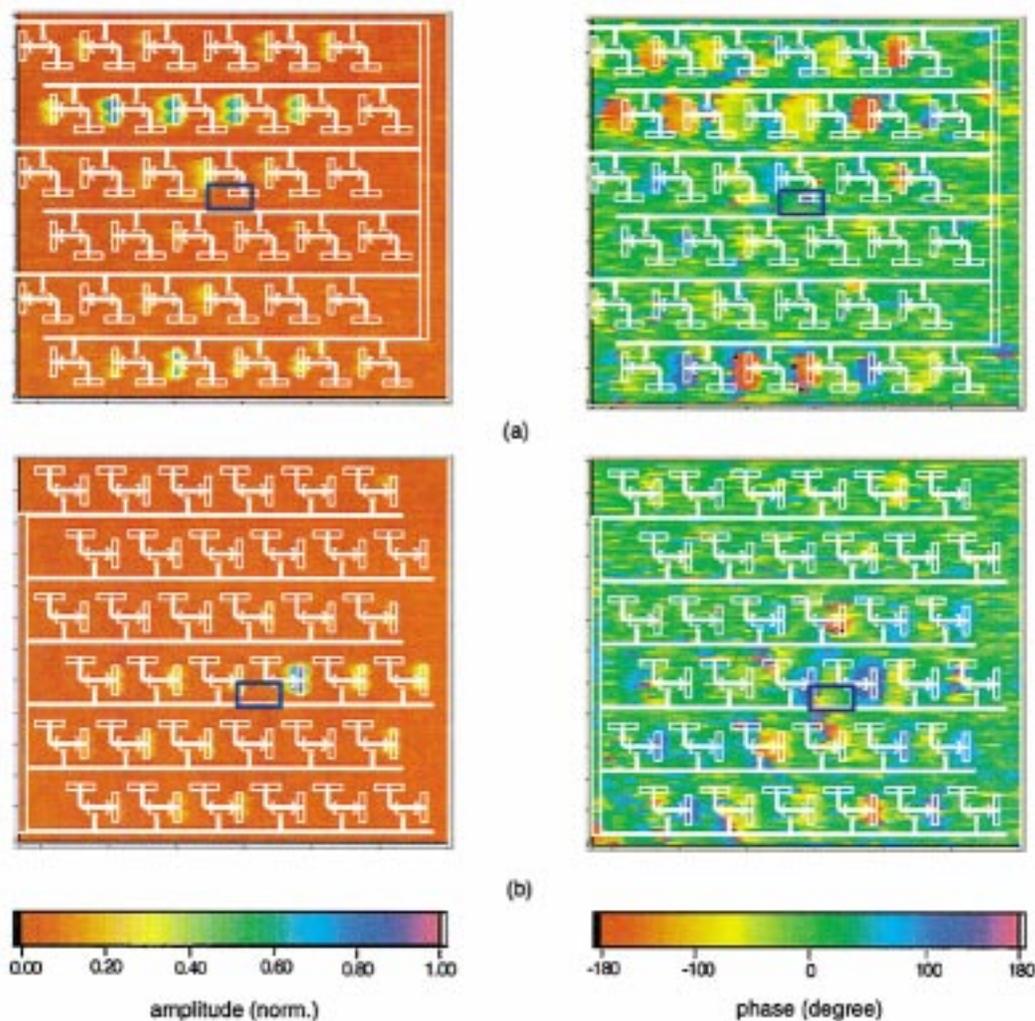
Fig. 9.   Coupling measurements with central element excited by waveguide feed, shown with a blue rectangle. Normalized amplitude (left-hand-side column) and phase (right-hand-side column) for (a) array A and (b) array B obtained by electrooptic measurements with a scan resolution of 500 μm × 450 μm. The total scan area is 6.3 cm × 5.4 cm.

surement results, as well as on the limited space for the feed in the electrooptic measurement setup, horn $H2$ was selected as the near-field feed for the QO arrays tested herein.

B. Slot Antenna Arrays

Two Ka-band slot antenna amplifier arrays with 36 elements each were fabricated on aluminum–nitride substrates with commercial low-power MMIC amplifiers in coplanar wave-guide (CPW) circuits, as described in detail in [19]. The two arrays differ in the biasing network only; the RF parts of the arrays are identical. For completeness, we list the microwave measurement results of these two arrays. The saturated output powers at 31 GHz were 0.3 and 0.5 W, with each MMIC contributing on average between 8.3 and 14 mW—this is 7 dB lower than the power specified by the manufacturer for a higher bias point. No liquid cooling was needed, and the AlN substrate reached a peak temperature of 40 °C. The average small-signal gain contributed by the MMICs was 10 and 14 dB, respectively, and was measured relative to a passive array. The measured far-field radiation patterns had bias on/off ratios of over 34 and 38 dB, and 3-dB beamwidths of about 10°.

The two different biasing schemes investigated were implemented as a direct result of an initial electrooptic-field-mapping diagnostic measurement on a previous embodiment of these arrays [8]. A cross-sectional view of the way in which this and subsequent measurements were performed is shown in Fig. 5, where the circuit side of the array is facing the feed horn and the probe scans the backside of the slots. The array is aligned to the radiation center of the feed horn using the results shown in Fig. 3, suggesting that electrooptic field mapping could also be applied for axial alignment of the elements of a quasi-optic system. The field image in Fig. 6, measured in the extreme near field of the array several hundred micrometers above its surface, shows that most of the functioning unit cells are concentrated nearest to the dc-bias bus bar for this first diagnostic array. This led to the conclusion that the biasing was nonuniform due to ohmic losses in the resistive ladder network consisting of the bias lines and internal biasing circuit of the MMICs [19]. Subsequent probe-station dc measurements showed a 5% error in the line of resistance as compared to the simple circuit-theory prediction. Based on this diagnosis, the bias lines for the two new arrays were redesigned for more uniform biasing. One array
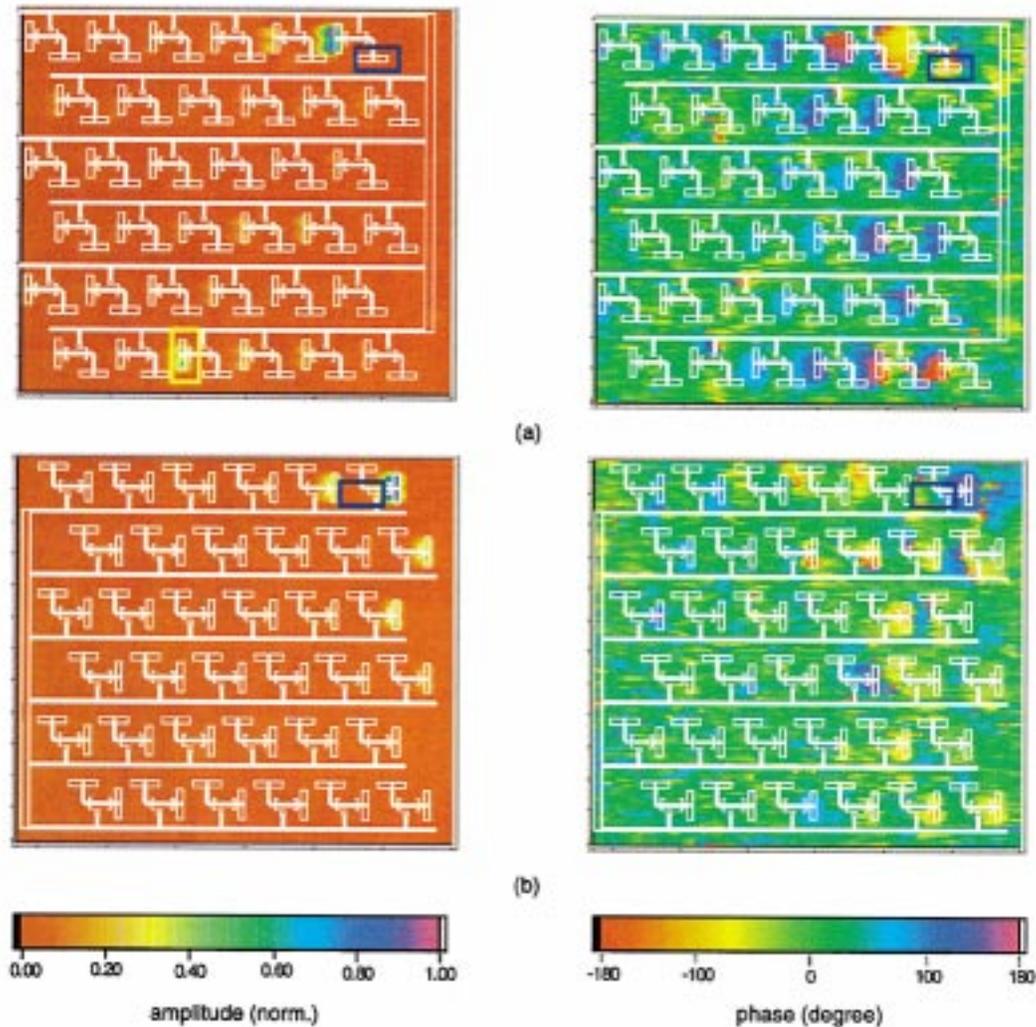
Fig. 10. Coupling measurements with edge-fed element. The waveguide feed is shown with a blue rectangle. The yellow rectangle shows the strongest coupled output power. Measured normalized amplitude (left-hand-side column) and phase (right-hand-side column) for (a) array A and (b) array B obtained by electrooptic measurements with a scan resolution of 500 μm $\times$ 450 μm. The total scan area is 6.3 cm $\times$ 5.4 cm.

(i.e., A) uses supplementary bias lines consisting of adhesive mylar and copper tape in order to reduce slot-line radiation and ohmic losses in the CPW bias lines. The second array (i.e., B) uses thicker bias metallization with additional air bridges and capacitors to suppress slot-mode radiation.

Several measurements were made on the two arrays. An extreme-near-field scan of the x-component of the electric field across a single output slot antenna element, approximately centrally located in array B (Fig. 7) shows proper operation of the second-resonant slot. There are two peaks in the radiation, symmetric with respect to the CPW feed, and the phase measurement shows in-phase operation of the two halves of the slot, as expected theoretically for this type of excitation.

Both arrays were fed with hard horn $H2$. The electrooptic scans of the electric-field component copolarized with the output slot antennas for arrays A and B are shown in Fig. 8. These scans show improvement over the first diagnostic array in terms of biasing uniformity and point out that the bias network design is critical to proper operation of large arrays as the number of elements increases. In this case, the biasing

scheme of array B provided better uniformity across the array due to reduced ohmic loss, as explained in [19]. This explains and confirms the difference in output power observed in the Ka-band far-field measurements for the two arrays.

Initially, some of the observed inconsistencies for arrays A and B were attributed to possible mutual coupling between array elements. Therefore, additional measurements have investigated inter-element coupling (isolation between cells) by exciting only a small part of the array. An open-ended Ka-band waveguide was positioned across one of the input slot antennas to provide the localized excitation. First, the open-ended waveguide was placed in the center of the array, as shown in Fig. 9 with a blue rectangle. The feed was then positioned at the edge of the array (Fig. 10). The edge and central elements see different boundary conditions and, therefore, the coupling in these two cases is expected to be different. The centrally-excited array A shows predominant coupling to the nearest row, whereas array B has more coupling to the nearest element in the same row. This is believed to be due to the fact that array B has more capacitors along the horizontal bias
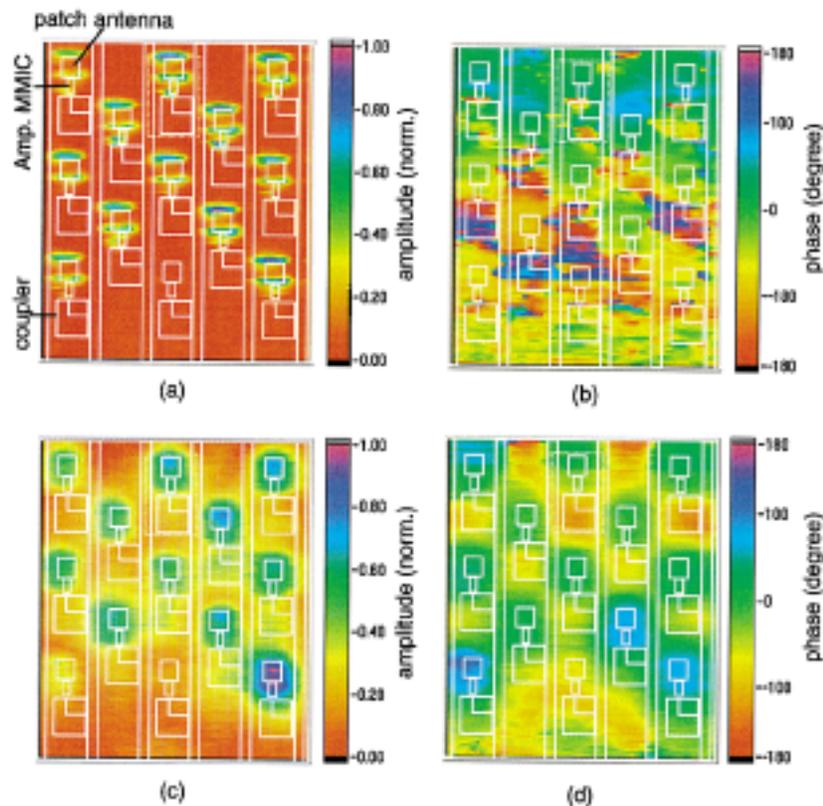
Fig. 11.   Electrooptic mapping result for the patch antenna array. (a) Normalized amplitude and (b) phase (in degrees) of the array for the y-component; measurement height: 0 mm. (c) Normalized amplitude and (d) phase for a measurement height of 1.2 mm ($\lambda/8$). The unit step size for the scanning was 284 μm $\times$ 341 μm, and 100 steps were taken for both the x- and y-directions. The total scan area covers 28.4 mm $\times$ 34.1 mm.

lines, preventing coupling in this direction. In the edge-excited case, array A shows an interesting build-up in coupling along a diagonal [see Fig. 10(a)] so that the farthest edge element from the excited unit cell is fully activated. This indicates that if coupling is not properly accounted for in the design, field can accumulate across the array due to the MMIC gain. This can result in nonuniform field distribution across the array, even if the cells are excited uniformly and have uniform gain. For example, in this case, the lower third element, shown in yellow in Fig. 10(a), is not at all excited directly by the wave radiated from the feed. In array B, this effect is not noticed because of the better isolation between the rows.

C. Amplifier Array Utilizing Patch Antennas

Another type of amplifier array, produced at Lockheed Martin, Orlando, FL, and using microstrip patch structures for the input and output antennas, has also been measured using the electrooptic field-mapping technique to examine the characteristics and performance of the array. This array has five columns of active cells, with three of those columns having four elements and the other two columns consisting of three elements. The array has two MMIC amplifiers per unit cell, one to amplify the input signal from the feed horn before it is coupled through the slot and the other one mounted right before the output patch antenna. In order to demonstrate the capability of this measurement technique to resolve the independent amplitude and phase of each active cell, scanning has been performed in the extreme near field only over the active area of the array.

For the measurement, horn $H2$ was again used as the feeding antenna [see Fig. 3(e) and (f)]. The unit step size for the scanning was 284 μm $\times$ 341 μm, and 100 steps were taken for both the x- and y-directions, resulting in a total scanning area of 28.4 mm $\times$ 34.1 mm. The same two types of crystals—BSO for the z-component and LiTaO$_3$ for the x- and y-components—were used to detect the three orthogonal electric-field components for this array.

Fig. 11 shows one of the measurement results obtained by electrooptic mapping. Fig. 11(a) and (b) displays normalized amplitude and phase (in degrees) of the y-component, which was the dominant field component for this array. The measurements are made at a height that is within several micrometers of the array surface. Due to the high spatial resolution of the electrooptic measurement technique, the two individual radiating edges of each patch antenna are easily distinguished in Fig. 11(a). The results also show a good agreement with previous measurements of a single patch antenna [15]. The field at a distance of 1.2 mm above the array, which corresponds to a distance of $\lambda/8$, is shown in Fig. 11(c) and (d).

It is quite noticeable that one element at the bottom of the middle column was malfunctioning. It was also found that this malfunctioning element disturbed the phase distribution for the array significantly [see Fig. 11(b)]. Despite the electric failure of this element, most of the patch antennas show a quite uniform phase distribution. These measurement results clearly demon-

strate the usefulness of the electrooptic field-mapping technique in carrying out fault isolation of array structures. The technique was quickly and easily able to demonstrate failure associated with an MMIC or a wire-bond connection.

Fig. 11(c) displays how the peak amplitude distributes uniformly over the entire patch structure. At this distance above the array ($\lambda/8$), the electric field generated from the two radiating edges [see Fig. 11(a)] is broadened enough to cover the whole antenna structure. Also, the effect of the malfunctioning element on the phase disturbance in areas extending away from the "off" element decreases significantly [see Fig. 11(d)]. As the distance from the array increases, the output electric field of the surrounding elements around the malfunctioning element stretches over the malfunctioning element. As a result, the absence of electric field above the malfunctioning element becomes less significant as the distance increases. Thus, we can predict that it is very difficult or even impossible to detect malfunctioning elements above a certain distance from the array. This phenomenon emphasizes the importance of accurate near-field measurements for validating the integrity of QO power-combining array structures. In other words, neither conventional far-field measurements nor low-resolution near-field measurement techniques are sufficient to isolate a problem *within* a unit cell of an array. In fact, for the system described in this section, verification of the unit cell design through detailed electrooptic field mapping encouraged the successful expansion of the array to one that has been demonstrated to radiate 25 W at Ka-band [2].

IV. CONCLUSION

The electrooptic field-mapping technique has been used for the diagnostic characterization of the extreme near-field pattern of several active amplifier arrays. The information obtained on the arrays and their hard-horn feeds has been proved to be vital for determining and understanding issues that could lead to the underperformance of such systems. For instance, through the electrooptic field maps, it has been confirmed that the hard horns exhibit outstanding amplitude and phase characteristics for plane-wave generation relative to the conventional WR-28 horn antenna. Furthermore, the measurements have revealed a number of important problems with the active arrays, such as a nonuniform dc bias, poor RF isolation performance, and malfunctioning MMICs.

In addition, the imaging of electric fields in the extreme near-field regime may be a completely novel way to "view" the interconnections within arrays, or even the layouts of operating RF circuits in general. The nearly real-time information made available by electrooptic field imaging could be especially valuable for troubleshooting and rectifying RF problem areas within production or prototype circuits, for validating internal design performance, or for analyzing failures in returned parts. Thus, the electrooptic field-mapping technique is a very powerful tool with which key physical insight can be attained into the operation of vitally important microwave systems.

REFERENCES

[1] N.-S. Cheng, T.-P. Dao, M. G. Case, D. B. Rensch, and R. A. York, "A 60-watt X-band spatially combined solid-state amplifier," in *IEEE MTT-S Int. Microwave Symp. Dig.*, New York, NY, 1999, pp. 539–542.

[2] J. Hubert, J. L. Mirth, S. Ortiz, and A. Mortazawi, "A 4-watt Ka-band quasi-optical amplifier," in *IEEE MTT-S Int. Microwave Symp. Dig.*, New York, NY, 1999, pp. 551–554.

[3] K. Yang, G. David, S. Robertson, J. F. Whitaker, and L. P. B. Katehi, "Electro-optic mapping of near field distributions in integrated microwave circuits," *IEEE Trans. Microwave Theory Tech.*, vol. 46, pp. 2338–2343, Dec. 1998.

[4] K. Kamogawa, I. Toyoda, K. Nishikawa, and T. Tokumitsu, "Characterization of a monolithic slot antenna using an electro-optic sampling technique," *IEEE Microwave Guided Wave Lett.*, vol. 4, pp. 414–416, Dec. 1994.

[5] T. Pfeifer, T. Loeffler, H. G. Roskos, H. Kurz, M. Singer, and E. M. Bieble, "Electro-optic near-field mapping of planar resonators," *IEEE Trans. Antennas Propagat.*, vol. 46, pp. 284–291, Feb. 1998.

[6] J. A. Valdmanis and G. Mourou, "Subpicosecond electro-optic sampling: Principles and applications," *IEEE J. Quantum Electron.*, vol. QE-22, pp. 69–78, Jan. 1986.

[7] B. H. Kolner and D. M. Bloom, "Electrooptic sampling in GaAs integrated circuits," *IEEE J. Quantum Electron.*, vol. QE-22, pp. 79–93, Jan. 1986.

[8] K. Yang, G. David, W. Wang, T. Marshall, L. W. Pearson, Z. Popović, L. P. B. Katehi, and J. F. Whitaker, "Electro-optic field mapping of quasioptic power-combining arrays," in *Opt. Soc. Amer. Ultrafast Electron. Optoelectron. Conf. Tech. Dig.*, Washington, DC, 1999, pp. 30–32.

[9] J. Nees and G. Mourou, "Noncontact electrooptic sampling with a GaAs injection laser," *Electron Lett.*, vol. 22, pp. 918–919, Aug. 1986.

[10] J. A. Valdmanis, "1-THz-bandwidth prober for high-speed devices and integrated circuits," *Electron Lett.*, vol. 23, pp. 1308–1310, Oct. 1987.

[11] S.-L. Huang, C. H. Lee, and H.-L. A. Hung, "Real-time linear time-domain network analysis using picosecond photoconductive mixer and sampler," *IEEE Trans. Microwave Theory Tech.*, vol. 43, pp. 1281–1289, June 1995.

[12] T. Pfeifer, H.-M. Heilinger, T. Löffler, C. Ohlhoff, C. Meyer, G. Lüpke, H. G. Roskos, and H. Kurz, "Optoelectronic on-chip characterization of ultrafast devices: Measurement techniques and applications," *IEEE J. Quantum Electron.*, vol. 2, pp. 586–604, Sept. 1996.

[13] H.-J. Cheng, J. F. Whitaker, K. J. Herrick, N. Dib, L. P. B. Katehi, and J. L. Coutaz, "Electro-optic probes: High-permittivity crystals versus low-permittivity polymers," in *Opt. Soc. Amer. Ultrafast Electron. Optoelectron. Tech. Dig.*, vol. 13, Washington, DC, 1995, pp. 128–130.

[14] X. Wu, D. Conn, J. Song, and K. Nickerson, "Invasiveness of LiTaO$_3$ and GaAs probes in external E-O sampling," *J. Lightwave Technol.*, pp. 448–454, Mar. 1993.

[15] K. Yang, G. David, J.-G. Yook, I. Papapolimerou, L. P. B. Katehi, and J. F. Whitaker, "Electrooptic mapping and finite element modeling of the near-field pattern of a microstrip patch antenna," *IEEE Trans. Microwave Theory Tech.*, vol. 48, pp. 288–294, Feb. 2000.

[16] M. A. Ali, S. Ortiz, T. Ivanov, and A. Mortazawi, "Analysis and measurement of hard horn feeds for the excitation of quasi-optical amplifiers," *IEEE Trans. Microwave Theory Tech.*, vol. 46, pp. 1469–1473, Oct. 1998.

[17] S. Hollung, A. E. Cox, and Z. Popović, "A bi-directional quasi-optical amplifier," *IEEE Trans. Microwave Theory Tech.*, vol. 45, pp. 2352–2357, Dec. 1997.

[18] C. A. Balanis, *Antenna Theory—Analysis and Design*. New York: Wiley, 1982.

[19] T. Marshall, M. Forman, and Z. Popović, "Two Ka-band quasi-optical amplifier arrays," *IEEE Trans. Microwave Theory Tech.*, vol. 47, pp. 2568–2573, Dec. 1999.

Kyoung Yang (S'90–M'92) was born in Seoul, Korea. He received the B.S. and M.S. degree in electrical engineering from the Seoul National University, Seoul, Korea, in 1990 and 1993, respectively, and is currently working toward the Ph.D. degree in electrical engineering and computer science at The University of Michigan at Ann Arbor.

His current research interests include the development of high-speed electrooptic and photo-conductive measurement technique for the characterization of microwave and millimeter-wave circuits and radiators.

Todd Marshall (S'97) received the B.S. degree in engineering physics, and the M.S. degree in electrical engineering from the University of Colorado, Boulder, in 1992 and 1996, respectively, and is currently working toward the Ph.D. degree in electrical engineering at the University of Colorado, Boulder.

From 1993 to 1994, he developed numerical models of light-trapping in solar cells at the National Renewable Energy Laboratory. His research interests include Ka-band free-space power combiners and electromagnetic modeling.

Michael Forman (S'95) received the B.S.E.E. and M.S.E.E. degrees from the University of Colorado, Boulder, in 1996 and 1998, respectively, and is currently working toward the Ph.D. degree in electrical engineering at the University of Colorado, Boulder.

His research interests include microwave and millimeter-wave power amplifiers, free-space power combiners, and K-band full-duplex amplifiers.

John Hubert received the M.S. degree from the University of Massachusetts, Amherst, in electrical and computer science.

In 1982, he joined Varian Associates, where he developed military radar components at SC-band. In 1986, he joined Lockheed Martin Missiles and Fire Control, Orlando, FL, where he focused on new technologies. He currently manages several research programs and also designs low-cost high-volume local multipoint distribution system (LMDS) transmitter and receiver modules. As a Technical Manager, his team of university professors and industry professionals developed the world's first QO amplifier to demonstrate power or gain at Ka-band. While with Lockheed Martin, he has developed over 250 MMIC chips up to W-band, several Ka-band modules, taught masters-level design classes, and marketed several startup companies. He has authored or co-authored numerous technical papers, contributed to masters-level college textbooks, and disclosed several patents.

Mr. Hubert currently sits on the University of Central Florida Engineering Advisory Board. He was the recipient of the Lockheed Martin Author of the Year Award, Award for Performance Excellence, a Team Award , and many Spot Awards. He was also the recipient of the IEEE Microwave Theory and Techniques Society (IEEE MTT-S) Quality Presentation Award.

Lee Mirth received the B.S.E.E. degree from Purdue University, West Layfayette, IN, and the M.B.A. degree from Syracuse University, Syracuse, NY.

He is currently a Research and Technology Manager for Millimeter Waves at Lockheed Martin Missiles and Fire Control, Orlando, FL, where his investigations include active and passive systems, with an emphasis on cost-effective applications and enabling technology. His experience includes silicon and gallium–arsenide component development and establishment of standards for both quality and reliability.

Zoya Popović (S'86–M'90–SM'99) received the Dipl.Ing. degree from the University of Belgrade, Belgrade, Yugoslavia, in 1985, and the Ph.D. degree from the California Institute of Technology, Pasadena, in 1990.

She is currently an Associate Professor of electrical engineering at the University of Colorado, Boulder. Her research interests include microwave and millimeter-wave QO techniques, microwave and millimeter-wave active antennas and circuits, and RF photonics.

Dr. Popović received the IEEE Microwave Theory and Techniques Society (IEEE MTT-S) Microwave Prize, the International Scientific Radio Union (URSI) Young Scientist Award, and the National Science Foundation Presidential Faculty Fellow Award in 1993. She was also the recipient of the URSI Isaac Koga Gold Medal in 1996 and the Humboldt Research Award in 2000 presented by the Alexander von Humboldt Foundation.

Linda P. B. Katehi (S'81–M'84–SM'89–F'95) received the B.S.E.E. degree from the National Technical University of Athens, Athens, Greece, in 1977, and the M.S.E.E. and Ph.D. degrees from the University of California at Los Angeles, in 1981 and 1984, respectively.

In September 1984, she joined the faculty of the Electrical Engineering and Computer Science Department, The University of Michigan at Ann Arbor, as an Assistant Professor, and then became an Associate Professor in 1989 and Professor in 1994. She has served in many administrative positions, including Director of Graduate Programs, College of Engineering (1995–1996), Elected Member of the College Executive Committee (1996–1998), Associate Dean for Graduate Education (1998–1999), and Associate Dean for Academic Affairs (since September 1999). She has authored or co-authored 410 papers published in refereed journals and symposia proceedings and she holds four U.S. patents. She has also generated 20 Ph.D. students.

Dr. Katehi is a member of the IEEE Antennas and Propagation Society (IEEE AP-S), the IEEE Microwave Theory and Techniques Society (IEEE MTT-S), Sigma Xi, Hybrid Microelectronics, and International Scientific Radio Union (URSI) Commission D. She was a member of the IEEE AP-S AdCom (1992–1995). She was an associate editor for the IEEE TRANSACTIONS ON MICROWAVE THEORY AND TECHNIQUES and the IEEE TRANSACTIONS ON ANTENNAS AND PROPAGATION. She was the recipient of the 1984 IEEE AP-S W. P. King (Best Paper Award for a Young Engineer), the 1985 IEEE AP-S S. A. Schelkunoff Award (Best Paper Award), the 1987 National Science Foundation Presidential Young Investigator Award, the 1987 URSI Booker Award, the 1994 Humboldt Research Award, the 1994 University of Michigan Faculty Recognition Award, the 1996 IEEE MTT-S Microwave Prize, the 1997 International Microelectronics and Packaging Society (IMAPS) Best Paper Award, and the 2000 IEEE Third Millennium Medal.

John F. Whitaker (S'84–M'88) received the B.Sc. degree in physics from Bucknell University, Lewisburg, PA, and the M.Sc. and Ph.D. degrees in electrical engineering from the University of Rochester, Rochester, NY.

In 1989, he joined the faculty of the Department of Electrical Engineering and Computer Science, The University of Michigan at Ann Arbor, where he is currently a Research Scientist and Adjunct Associate Professor, and the Coordinator of the Ultrafast Technology Area in the National Science Foundation (NSF) Center for Ultrafast Optical Science. In 1995, he was a Visiting Professor (First Class) at the University of Savoie, Savoie, France. His research interests involve ultrafast-response optoelectronic materials, devices, and test and characterization techniques, as well as guided and free-space-radiating terahertz-bandwidth pulses.

Dr. Whitaker is a member of IEEE Microwave Theory and Techniques Society (IEEE MTT-S) and IEEE Lasers and Electro-Optics Society (IEEE LEOS). He is currently the chair of the IEEE LEOS Technical Committee on Ultrafast Optics and Electronics. He was a recipient of the 1996 Microwave Prize presented by the IEEE MTT-S. He also received the Research Excellence Award presented by the Department of Electrical Engineering and Computer Science, The University of Michigan at Ann Arbor, and the Outstanding Research Scientist Achievement Award presented by the College of Engineering, The University of Michigan at Ann Arbor.